Revisions from Conterence Paper highlighted,

Temperature Dependent Modal Test/Analysis Correlation of X-34 Fastrac Composite

Rocket Nozzle

Andrew M. Brown*

Visiting Professor, Department of Mechanical Engineering, UNC Charlotte, Charlotte, NC 28223

Aerospace Engineer, Structural Dynamics and Loads Group, NASA/Marshall Space Flight Center, MSFC, Al 35812

Abstract

A unique high temperature modal test and model correlation/update program has been performed on the composite nozzle of the FASTRAC engine for the NASA X34 Reusable Launch Vehicle. The program was required to provide an accurate high temperature model of the nozzle for incorporation into the engine system structural dynamics model for loads calculation; this model is significantly different from the ambient case due to the large decrease in composite stiffness properties due to heating. The high-temperature modal test was performed during a hot-fire test of the nozzle. Previously, a series of high fidelity modal tests and finite-element model correlation of the nozzle in a free-free configuration had been performed. This model was then attached to a modal-test verified model of the engine hot-fire test stand and the ambient system mode shapes were identified. A reduced set of accelerometers was then attached to the nozzle, the engine fired full-duration, and the frequency peaks corresponding to the ambient nozzle modes individually isolated and tracked as they decreased during the test. To

update the finite-element model of the nozzle to these frequency curves, the percentage differences of the anisotropic composite moduli due to temperature variation from ambient, which had been used in the initial modeling and which were obtained by small sample coupon testing, were multiplied by an iteratively determined constant factor. These new properties were used to create high-temperature nozzle models corresponding to 10 second engine operation increments and tied into the engine system model for loads determination.

Introduction

The X34 air-launched hypersonic rocket-plane is a technology demonstrator vehicle being built as part of the NASA Reusable Launch Vehicle program. The goal of the X-34 program is to demonstrate new technologies that can be used to reduce the cost of access to orbit from \$10,000/lb to \$1000/lb. The FASTRAC engine is being designed, analyzed, manufactured, and tested as the main engine for that vehicle. The engine uses a gas-generator turbopump cycle fueled by Lox-Kerosene and is rated to 60,000 lb. of thrust. It is designed to be built at a much lower cost than conventional engines, with a small part count, simple assembly procedure, and a rapidly manufactured two-layer composite integral combustion chamber/nozzle (Fig.1).

Large dynamic loads propagate through the engine due to rocket combustion and from the turbopump. In order to predict the values of these loads for design and analysis, an accurate dynamic finite-element model of the engine is required (MSC/Patran® and MSC/Nastran® were used for all analyses). The structural backbone of this engine is the nozzle, which all the other components are mounted upon, as seen in Figure 2. This nozzle is made of a two-layer composite composed of a silica phenolic liner and a graphite epoxy overwrap, presenting new challenges in modeling and testing. The first of these was generating a 360° finite-element dynamic model

that could be built and correlated in a timely fashion to allow for multiple nozzle and engine test configurations. This correlation effort was made considerably more difficult because of the anisotropy of the composite materials. This effort has been documented in a previous paper by the author¹.

Another major challenge became clear when it was realized that the dynamic stiffness properties of the nozzle liner would change substantially during the firing of the engine, thereby changing the loads throughout the engine. This change was because of the large temperature-dependence of the Young's Moduli and Poisson's ratios of silica phenolic, which had been obtained from coupon testing. Initial predictions of the changes in natural frequencies, presented in Ref. 1, indicated a possible decrease of over 40% by the end of the engine burn. Since this was based on predictions of not only high-temperature material properties but on predictions of temperatures, it was clear that a test to verify the actual dynamic properties would be necessary. The determination of the type of test, test description, and correlation to the test are the subjects of this paper.

There has been a limited amount of work previously published on this subject. In 1991, Kehow and Snyder performed a detailed experimental and analytical study of aluminum plate specimens which were heated uniformly, nonuniformly, and transiently. The finite-element method was used as the analytical baseline for comparison with the experimental results. They found that the natural frequencies decreased, the mode shapes stayed constant, and the damping for some of the modes increased². The fact that the mode shapes stayed constant was an important result since it implies that the bulk of the effect of the heating was limited to an easily modeled change in the elastic modulus rather that some unknown combination of changes in the modulus and density. In 1993, Kehow and Deaton followed this study up with similar tests and

analysis on titanium and fiberglass plates³. Some of the important conclusions from this study were that the reduction in material properties due to heating was the primary factor in changes in dynamic characteristics for uniform heating, but that thermal stresses played an equally important role for nonuniform and transient heating. A closed-form analytical solution for a heated anisotropic plate with specified boundary conditions was presented by Locke in 1994 which also compared favorably with finite-element analysis⁴. To the author's knowledge, the study described in the paper is the first published work describing large scale modal testing and model correlation of complex structures undergoing a significant amount of heating that are composed of materials whose dynamic properties are strongly dependent on temperature.

Approach

A variety of options were discussed for implementation of the test/analysis correlation. The first one considered was to heat the nozzle in large ovens able to cover the expected temperature range. A method for remotely controlling impacts and obtaining acceleration measurements was formulated to perform the modal test in the oven. In the end, however, it was realized that creating an appropriate thermal distribution throughout the nozzle in the oven was impractical. In addition, the temperature of the graphite epoxy overwrap was not predicted to exceed 200°F during engine burn, and this could not be controlled in the oven. A solution to the problem became apparent when plans were made independently to perform a hot-fire test of the nozzle itself without any other engine hardware to satisfy a variety of programmatic goals. This test would be full duration, the temperatures experienced by the nozzle would be the same as expected in an actual mission engine burn, and the nozzle would be isolated from most of the surrounding hardware, which was critical for a reasonable correlation with the detailed nozzle-

only model. A decision was therefore made to use this hot-fire test to obtain the modal data needed for finite-element model correlation.

The plan for the test and correlation consisted of several steps. Initially, a model of the test-stand was built to provide accurate boundary conditions for the nozzle, which would be cantilevered off of it. The model was not intended to rigorously simulate every mode of the stand, but rather just to provide a reasonable model of the interface with the nozzle. A modal test of the stand was performed (see Fig. 3), and the stand model was correlated to some degree, as shown in Table 1.

The next step was to perform an ambient temperature test-stand-nozzle modal test and model correlation. This test was used to identify the modes and natural frequencies of the system that would exist at the beginning of the engine fire. This modal test would verify the model of the test stand combined with a previously free-free modal test verified model of the nozzle. This test was performed immediately before the hot-fire, but a quick look at the data suggested that the combined structural system introduced families of modes for one of the nozzle's primary modes, first bending, which existed only as a single mode for the nozzle in its free-free configuration (see Fig. 4). This family consisted of different modes where sections of the test stand, such as the front mounting plate, would move in or out-of-phase with the nozzle first bending. These modes were so numerous that it would be very difficult to update a finiteelement model to match them. Fortunately, the nozzle nodal diameter modes remained somewhat isolated from the interface with the boundary condition (Fig. 5). This allowed the hotfire modal test plan to proceed, where only the nodal-diameter modes of the nozzle-test stand model would be used for correlation. These modes are not sufficient by themselves for correlating a model since the nodal diameter modes do not fully account for the effect of the

longitudinal Young's Modulus E_L (which is independent of the Young's Moduli in the other directions), so this process forced an assumption that the temperature effects on the other material constants were also applicable to E_L .

Hot-Fire Test

The plan for the hot-fire modal test would be to only measure the response using a subset of the number of accelerometers needed for a full-scale modal test, since the available instrumentation channels were limited due to the other requirements of the test. Special precautions had to be taken to ensure that the accelerometers would stay on the nozzle and would not burn up. Fortunately, since the accelerometers were installed on the external surface of the nozzle, which was not expected to exceed a temperature of 200° F, merely covering them with fire-tape was adequate. Since the excitation, which would be generated by the combustion process itself, could not be measured, Power Spectral Density (PSD) plots of the acceleration response only would be obtained, with peaks occurring at the natural frequencies of the system since there were no pure harmonic forcing functions that would show up independently. These peaks would be tied to their appropriate mode shapes at the initiation of the test using the preliminary ambient temperature modal test results described above. PSD's would be obtained at frequent time intervals throughout the test, and by combining these plots into a "waterfall" plot, the change in the frequency of the peaks with respect to time can be seen. To verify that the frequencies being tracked were the natural frequencies of the specific mode shapes being sought, the PSD's of the different accelerometer locations would be compared to obtain rough mode shapes.

The hot-fire test was performed in late November 1998. Several measures of data quality were performed, and only 2 of the 12 accelerometers apparently debonded from the nozzle. Examination of the waterfall plots of the remaining instruments showed that the frequency peaks were clearly defined and could be tracked as planned. The time history of each frequency peak was then extracted from the waterfall plots for model correlation. The history for one of these accelerometers tracking the fundamental two nodal-diameter mode of the nozzle is shown in Fig. 6. In addition, comparison of the relative magnitudes for different accelerometers verified that the mode shapes associated with the peaks were the ones obtained from the ambient modal test and that the proper mode was being tracked.

Thermal Model

An essential step in the modeling procedure was applying the correct temperature to the different locations in the nozzle as it heats up during the test. This information was obtained by using temperature probes during the test to correlate a thermal model of the nozzle, which had been built previously and was used for the initial estimates of the natural frequency decline.

After this thermal correlation was completed, a complete profile of the average bulk temperature of the inner composite layer for each axial position of the nozzle at 0, 25, 50, 100, and 150 seconds into the test was generated (since there was very little difference between the values at 100 and 150 seconds, the 100-150 second increment was ignored at this point). A plot of these temperatures versus the axial location along the nozzle is shown in Fig. 7 (a cross-section of the nozzle is also superimposed for illustrative purposes). The bulk value was chosen since two-dimensional composite plate elements were used in the finite-element model, so temperature variation in the transverse direction would not be able to be used. Using a linear interpolation

between these time profiles, the temperature at any location at any time into the test was generated.

Model Correlation

Any of a number of methods could be now applied to obtain the desired test-verified "hot" model of the nozzle. Previous work discussed earlier indicates that both the variation in stiffness properties and the thermal stress play a role in the change in natural frequencies for the transient heating conditions that existed in the hot-fire test, but for simplification and timeliness it was originally assumed that the material properties were solely responsible for the change. This assumption has been verified after the completion of the engine program by performing a complete non-linear modal analysis, which incorporates the effect of the thermal stresses due to the differential heating of the nozzle. Coefficients of thermal expansion as a function of temperature obtained from coupon testing were first transformed to the finite-element coordinate system as explained in Ref. 1. The transformed properties were then input into the model according to the nozzle temperature distribution at 100 s, which had been obtained from the hot-fire test. The non-linear modal analysis was then performed, and the results were almost identical to those when the thermal stress effect was ignored, with a 2.9% increase for the fundamental nozzle mode and decreasing errors for higher frequency modes.

The correlation was therefore obtained solely by perturbing the original material modulus properties vs. temperature chart until a "reasonable" level of model/test agreement was achieved. Of course, the definition of "reasonable agreement" with test is subject to considerable variation. In this case, the frequencies for several of the higher modes were not in agreement even at the beginning of the test, so it would not make sense to try to exactly match the frequencies at the

end. It was decided instead to try to match the rate of decline in natural frequency to obtain the true effect of the temperature. The most straightforward method to achieve this goal was to multiply the percent decrease at a particular temperature of all the properties from their baseline value at 70°F by some constant. After several iterations, a factor of 1.2 was determined for all the properties but Poison's ratio υ , which required a factor of 1.05. The results of applying this factor on the material properties is shown in Table 2.

Table 3 shows the final natural frequency test/analysis comparisons after model correlation, and Fig. 8 shows the decline of each of the modes (analytically and experimentally) versus time into the test. The modal descriptions in the chart legend are 2ND for the 2 nodal diameter mode, 3ND, etc. and the "Balloon 2ND" refers to a mode which has a 2 nodal diameter shape just aft of the throat in addition to another 2 nodal diameter shape out-of-phase with it near the exit plane. Final correlation consisted of qualitatively matching the test/analysis frequency curves as well as using the quantitative error measures.

Model Implementation

Using the newly correlated material property versus temperature profile and the new nozzle location temperature profiles, complete nozzle models representing the material properties at 10 second increments into hot-fire were then generated. These models were supplied to the total engine system model for loads generation at these increments, which is discussed in a paper by Frady.⁵

Sources of Error

There are several sources of error in this correlation procedure. Discrepancies probably exist due to some modeling errors as discussed in Ref. 1, the lack of good longitudinal test modes to correlate E_L to, and the scaling method used to alter the material properties table. In addition, the transverse variation in temperature was not accounted for; evaluation of the magnitude of this error could be estimated by comparison with a solid finite-element model of the composite, which has not been performed here. However, the final results indicate that no large inconsistencies exist within the model itself (which can occur by locally varying stiffnesses to match test data, for instance), and that a usable high-temperature model was created that matches the modal properties during hot fire. Since the original model (at ambient temperature conditions) had been test-verified with an extensive series of tests, and the thermal distribution was also derived from a test-verified model, the error in the small-sample coupon measurements from the as-built case seemed to be the most likely source of discrepancy. The assumptions used also allowed the creation of this model in a timely fashion, which was important since it was critically needed for engine system loads analysis.

Conclusion

A unique high-temperature modal test and finite-element model correlation/update program was performed on the X-34 FASTRAC composite rocket nozzle for loads prediction during engine operation. The modal test was actually performed as part of a standard full duration hot-fire test of the nozzle by itself, which simulated the actual operation of the FASTRAC engine. A detailed preliminary series of modal tests of the structural components of the nozzle/test stand system was first performed at ambient conditions to baseline the modes and natural frequencies. "Waterfall" PSD plots using a reduced set of accelerometers were then used

to track the modes during the hot-fire test. The finite-element model was updated to match the decline in natural frequencies by scaling the decrease of the predicted material property for each temperature. The temperature distribution of the model was obtained by using a thermal model of the nozzle that was also correlated from the same hot-fire test. The new material property curves were used to create a series of high-temperature models representing the structural dynamic characteristics of the engine at 10 second increments into operation. These models were then tied into the structural dynamic model of the entire engine for interface dynamic loads calculation. This approach can potentially be generalized as a method for correcting modulus vs. temperature coupon testing to actual composite layups.

References

¹ Brown, A. M., Sullivan, R, "Dynamic Modeling and Correlation of the X-34 Composite Rocket Nozzle," NASA/TP-1998-208531, July 1998

²Snyder, H.T., Kehoe, M. W., "Determination of the Effects of Heating on Modal Characteristics of an Aluminum Plate With Application to Hypersonic Vehicles," NASA Technical Memorandum 4274, 1991

³ Kehoe, M. W., Deaton, V.C, Correlation of Analytical and Experimental Hot Structure Vibration Results," NASA Technical Memorandum 104269, 1993.

⁴Locke, J.E., "Vibration Analysis of Heated Anisotropic Plates with Free Edge Conditions," Journal of Aircraft, Vol. 31, No. 3, May-June 1994, pp. 696-702.

⁵Frady, G. "Engine Systems Loads Development for the Fastrac 60-K Flight Engine," 2000 AIAA Structures, Structural Dynamics, and Materials Conference, April 3-6, 2000, Atlanta, Georgia, AIAA Paper #2000-1612.

Table 1 Test Stand Only Test/Analysis Comparison

_Mode	Description	Analysis (hz)	Test (hz)		
1	Main Structure, front plate side to side	24.0	23.8		
2	Predominantly plate up & down	48.4	50.0		
3	Plate diagonal twisting about vertical axis	61.54	68.51		

Table 2 Original and Altered Composite Material Constants as a Function of Temperature

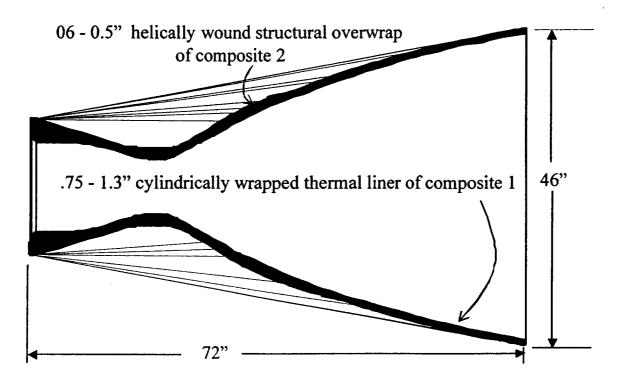
Original Properties												
Temperatu			E norm	υ	ນ norm-	11 norm	C	C	CEIL			
re (°F)	/1000	/1000	/1000	warp-	warp	fill	G warp- fill /1000	G warp-	G fill-			
	(psi)	(psi)	(psi)	fill	waip	IIII	(psi)	norm /1000	norm /1000			
		(F31)	(p 0.)				(psi)	(psi)	(psi)			
70	2810	2810	2000	0.18	0.21	0.21	894	535	535			
250	2690	2690	1400	0.14	0.19	0.19	850	438	438			
350	2440	2440	1080	0.12	0.19	0.19	596	401	401			
400	2360	2360	780	0.1	0.18	0.18	484	322	322			
450	2280	2280	540	0.08	0.17	0.17	413	253	253			
500	2190	2190	292	0.07	0.16	0.16	340	177	177			
550	2090	2090	224	0.07	0.15	0.15	324	166	166			
600	2010	2010	177	0.06	0.14	0.14	316	153	153			
750	1800	1800	102	0.05	0.11	0.11	273	146	146			
900	1660	1660	59.9	0.04	0.1	0.1	256	151	151			
1050	1510	1510	51.5	0.04	0.1	0.1	245	159	159			
1200	1350	1350	50.8	0.04	0.1	0.1	245	179	179			
1500	1090	1090	51.6	0.04	0.12	0.12	207	199	199			
								<u> </u>	···			
	Altered Properties											
factor on	1.2	1.2	1.02	1.2	1.2	1.2	1.2	1.2	1.2			
slope												
70°F	2810	2810	2000	0.18	0.21	0.21	894	535	535			
250	2666	2666	1388	0.132	0.186	0.186	841.2	418.6	418.6			
350	2366	2366	1062	0.108	0.186	0.186	536.4	374.2	374.2			
400	2270	2270	755.6	0.084	0.174	0.174	402	279.4	279.4			
450	2174	2174	510.8	0.06	0.162	0.162	316.8	196.6	196.6			
500	2066	2066	257.8	0.048	0.15	0.15	229.2	105.4	105.4			
550	1946	1946	188.5	0.048	0.138	0.138	210	92.2	92.2			
600	1850	1850	140.5	0.036	0.126	0.126	200.4	76.6	76.6			
750	1598	1598	64.04	0.024	0.09	0.09	148.8	68.2	68.2			
900	1430	1430	21.1	0.012	0.078	0.078	128.4	74.2	74.2			
1050	1250	1250	12.53	0.012	0.078	0.078	115.2	83.8	83.8			
1200	1058	1058	11.82	0.012	0.078	0.078	115.2	107.8	107.8			

Table 3 Final Comparison of Test and Analytical Natural Frequencies

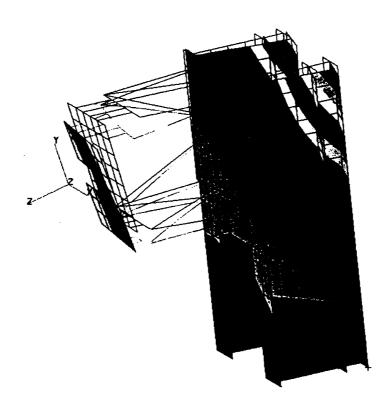
Mode	Test @ 0 sec.	Analyti cal @ 0 sec	1	Test @ 25 sec.		Error	Test @ 50 sec.		Error		Analyti cal @ 100 sec	% Error
2 Nodal Diam.	45.5	46.7	-3%	37.3	40.3	-8%	35	37.7	-8%	32.7	33.3	-2%
3 ND	113.4	118.3	-4%	94.5	99.2	-5%	88.5	95.4	-8%	81.4	83.2	-2%
4 ND	210.4	221	-5%	177.2	183.7	-4%	165.5	176.6	-7%	154	154	0%
5 ND	334.4	357	-7%	284	293.3	-3%	265	280.2	-6%	244	243.8	0%
Balloon 2ND	385	357	7%	357.5	325.7	9%	344	291.6	15%	330	264.1	20%

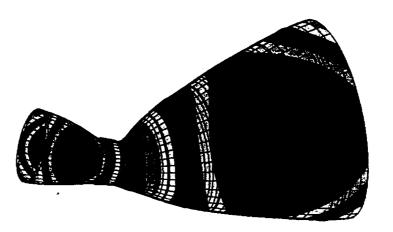
List of Figures

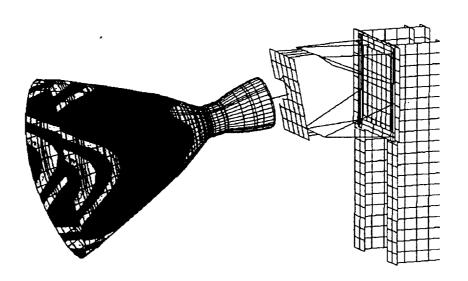
- Fig. 1. Cutaway of X-34 FASTRAC rocket nozzle
- Fig. 2. Turbopump and other FASTRAC components counted on nozzle
- Fig. 3. Test stand, mode 2 at 50Hz (deformed shape superimposed on undeformed shape).
- Fig. 4. Nozzle, free-free, first bending at 180.9 Hz.
- Fig. 5. Two nodal diameter (ND) mode of nozzle on test stand.
- Fig. 6. Isolated time history trace of two ND mode frequency peak for accelerometer 11.
- Fig. 7. Temperature of nozzle for various times into hot-fire test vs. axial location.
- Fig. 8. Comparison of variation in natural frequencies versus time into hot-fire between test and correlated analytical results.











.

